SF2A 2007
J. Bouvier, A. Chalabaev, C. Charbonnel (eds)

DYNAMICAL PROCESSES IN THE SUBSURFACE LAYERS OF THE SUN.

S. Lefebvre[1], P. Nghiem[1] and S. Turck-Chièze[1]

Abstract. Recent results obtained by Lefebvre and Kosovichev (2005) using f-modes frequencies from SOHO/MDI, indicate a change in the stratification of the subsurface layers, more precisely a non-homogeneous variation of these layers with depth and time. To progress on this transition zone between the solar interior and the external part, we begin to analyse the problem from a theoretical point of view. Using the CESAM code, we show how a small variation in the radius implies a variation in the subsurface structure. We use the theoretical f-modes frequencies to examine the corresponding changes in the stratification. Furthermore, we discuss the related physics, very complex in this zone, and show the variations of the temperature gradients, the density and pressure scale heights caused by the change in radius.

1 Introduction

Recently, Lefebvre & Kosovichev (2005) and Lefebvre et al. (2007) reported changes with the solar cycle of the solar subsurface stratification using inversion of SOHO/MDI f-mode frequencies. Their computations demonstrate a variability of the position of the subsurface layers, which is localized in a double-structure layer centered at 0.99 $R_{\odot}$ and is extended to the surface. These changes are not uniform with depth: in the deepest part, between 0.97 and 0.99 $R_{\odot}$, the position of the layers varies in phase with the solar cycle, whereas it is the opposite in the uppest part, above 0.99 $R_{\odot}$, where the variability is in antiphase.

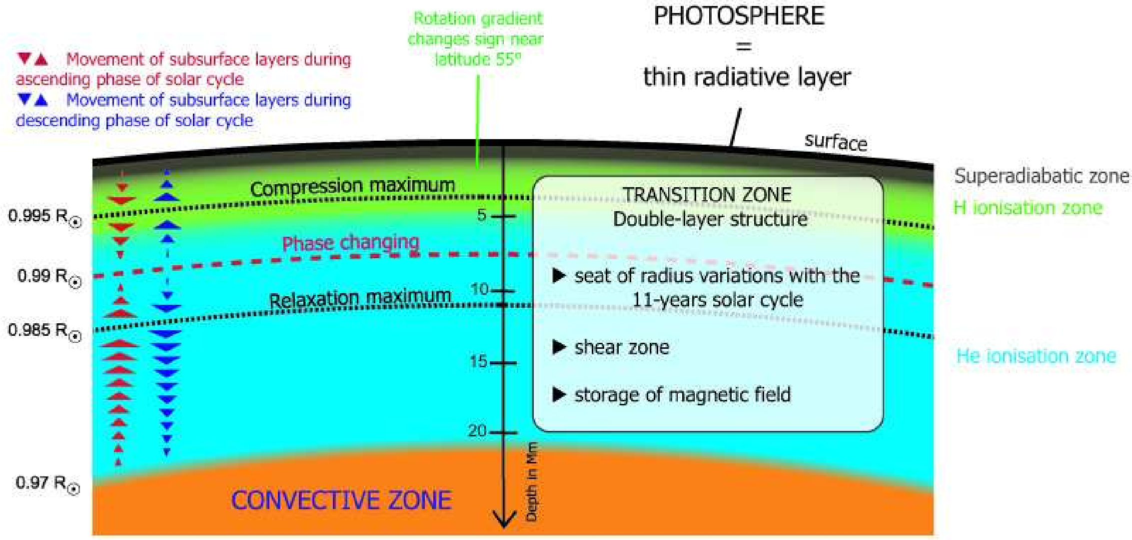

Fig. 1. Schematic view of the leptocline (non-scale scheme).

Despite a long lack of interest by scientists for these subsurface layers due to their complexity and negligible mass, this zone newly attracts due to the emergence of the space weather science (Rozelot et al. 2006) and the

[1] Laboratoire AIM, CEA/DSM-CNRS-Université Paris Diderot, DAPNIA/SAp, 91191 Gif sur Yvette, France

need to couple the internal dynamics to the solar atmosphere. Figure 1 introduces a scheme of these zone, above 0.96 $R_\odot$, the so-called *Leptocline* (Godier & Rozelot 2001). Its physics is complex: seat of the radius variation with the 11-year cycle (Lefebvre & Kosovichev 2005), potential storage zone for the magnetic field (Nghiem et al. 2006), intense shear zone with hydrogen and helium partial ionisation zones. This paper is devoted to the presentation of a theoretical work in the framework of classical stellar modelling in order to compare with observational data. Future objectives are to introduce the local effect of magnetic field. We choose to use solar models to examine the effect of a variation of the calibrated radius and luminosity on the structure beneath the photosphere. The theoretical f-mode frequencies and the same inversion procedure described in Lefebvre & Kosovichev (2005) permit to show that changes in the solar subsurface are related to variations in the solar radius.

2 Model computations

We use the CESAM evolution code (Morel 1997) to calibrate several models M_i at chosen solar radii R_i and luminosities L_i. We choose to examine both the effect of a radius and luminosity change on subsurface physics. We computed five cases listed in Table 1. M_1 is considered as the reference model (Couvidat et al. 2003; Turck-Chièze et al. 2001) with $R_1 = R_\odot$ and $L_1 = L_\odot$. The other models M_i, for $i = 2...5$, are built according to a ratio for the calibrated radius $\frac{R_i}{R_\odot} = 1.0000 \pm 0.0002$ and the calibrated luminosity $\frac{L_i}{L_\odot} = 1.000 \pm 0.001$. We considered the differences between these models and computed 4 cases: $M_i - M_1$ for $i = 2...5$. The aim is to mimic variations of the radius and luminosity that supposedly happen during the 11-year solar activity cycle. The relative change in the luminosity of 10^{-3} is similar to that of the observed solar irradiance during the cycle. The relative variations for the radius are certainly larger than the observed ones during the solar cycle but we prefer to place ourself at a level well above the numerical precision of the CESAM code.

The evolution of the following parameters are studied: the mass m, the temperature T, the density ρ, the pressure p, the sound speed c, the adiabatic exponent $\Gamma_1 = (\frac{d\ln p}{d\ln\rho})_{adia}$, the density scale $H_\rho = -\left(\frac{d\ln\rho}{dr}\right)^{-1}$, the pressure scale $H_p = -\left(\frac{d\ln p}{dr}\right)^{-1}$, the radiative temperature gradient $\nabla_{rad} = \frac{d\ln T}{d\ln p}$, the real temperature gradient $\nabla_{real} = min(\nabla_{rad}, \nabla_{adia})$, the opacity κ and the gravitational energy Eg.

Table 1. List of calibrated models .

Model	R^a	$R/R_\odot$	L^b	$L/L_\odot$
1	6.9599	1.0000	3.8460	1.0000
2	6.9613	1.0002	3.8499	1.0010
3	6.9613	1.0002	3.8422	0.9990
4	6.9586	0.9998	3.8499	1.0010
5	6.9585	0.9998	3.8422	0.9990

Model 1 is considered as the reference model (Couvidat et al. 2003; Turck-Chièze et al. 2001).
[a] ($\times 10^5$ km)
[b] ($\times 10^{33}$ ergs s^{-1})

Figures 2 show the evolution with depth of the previous quoted parameters when computing the differences[1] between models as described above. The study is restricted to the zone between 0.96 $R_\odot$ and 0.998 $R_\odot$. Most of these parameters present important variations in this region:

- The change in luminosity has negligible effects at the surface because such a change come from variations in the nuclear core contrary to the cycle change which probably comes from more external layers.
- The behaviors of c, H_p and H_ρ are almost the same i.e. a bump around 0.99 $R_\odot$ with opposite variations between M_2, M_3 and M_4, M_5.

[1]The differences here are computed by reporting each fractional radius x_i to the reference radius, i.e. $x_i^{new} = x_i R_i / R_{ref}$; in this case, all models are in the same referential.

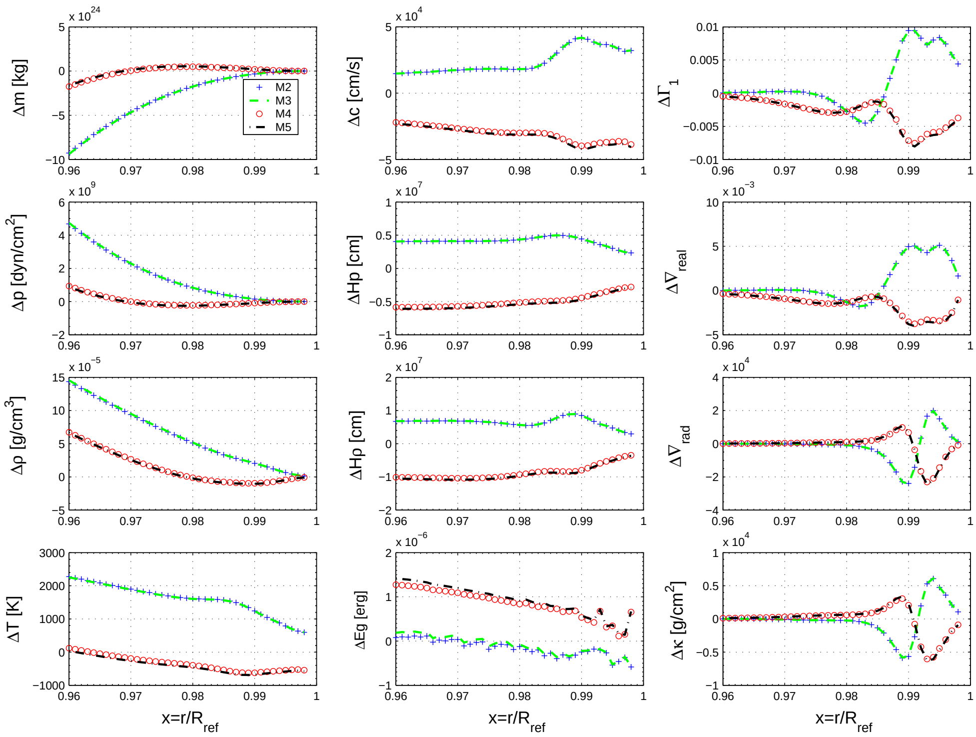

Fig. 2. Evolution of physical parameters when computing the difference between a standard solar model and four other models calibrated with a combination of two radii and two luminosities (see text).

- The differences of Γ_1 and ∇_{real} have similar variations and present a double peak near 0.99 $R_\odot$ with almost equal amplitude.
- The variations of ∇_{rad} and κ present a sign change at 0.99 $R_\odot$, connected to the partial ionisation of the light elements.
- There is no particular behavior concerning the variation in mass, density, pressure and energy Eg.

These first trends indicate that the subsurface layers are strongly affected by a change in the radius. In the next section, we completed the study by the analysis of f-mode frequencies issued from these models.

3 Numerical inversion of theoretical f-mode frequency

3.1 Variation of the theoretical f-modes

Using the ADIPLS code (Christensen-Dalsgaard 1982), we compute for each model the theoretical f-modes frequencies: the relative differences of frequencies by reference to M_1 are plotted in Fig. 3. As the difference is small, we choose to plot the absolute value of the difference, keeping in mind that the difference of frequencies between M_2 and M_1, and between M_3 and M_1, is negative. A quick analysis of this graph shows us that the relative difference is decreasing up to $\approx 1300 \mu Hz$ and is increasing after. The next paragraph will demonstrate that this behavior comes from changes in the subsurface stratification.

3.2 Inversion and results

We use the same procedure published in Lefebvre & Kosovichev (2005) to infer the changes in the position of subsurface layers from the f-mode frequency variations. The relation between the relative frequency variations $\delta\nu/\nu$ for f-modes and the associated Lagrangian perturbation of the radius $\delta r/r$ of subsurface layers has been

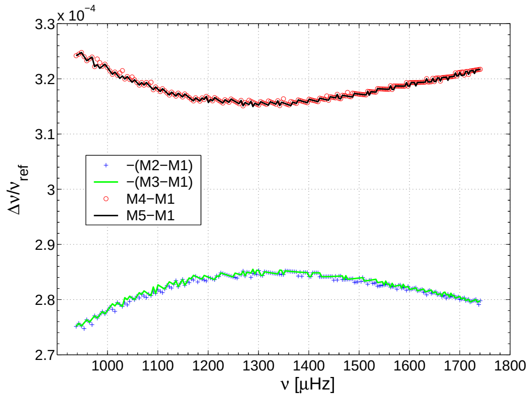

Fig. 3. Relative difference of f-modes frequencies between M_i and M_1 for $i = 2...5$.

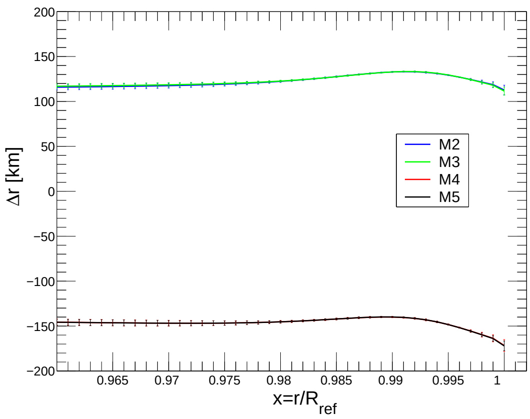

Fig. 4. Radial variation Δr as a function of the fractional radius $x = r/R_{ref}$, obtained by inversion of eq. 3.1. Note the behavior of the curves near $x = 0.99$. The error bars are the standard deviation after averaging over a set of random noise added to the relative frequencies reconstructed in Fig. 5.

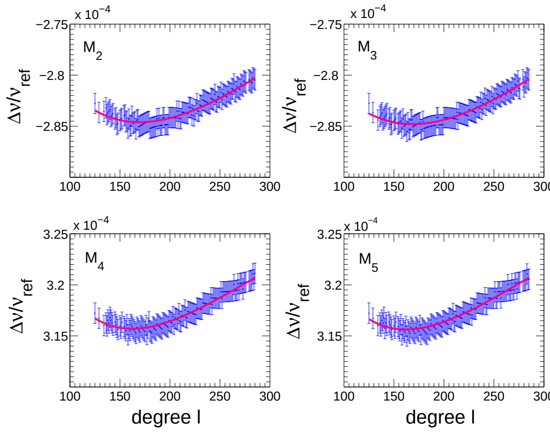

Fig. 5. For each model, $\Delta\nu/\nu_{ref}$ as a function of the degree l. The reference is model M_1 and errors have been artificially added to the data, such as $\sigma = 1 \times 10^{-6}$. The solid curves are the result of direct integration of Eq. 3.1, providing the solutions in Fig. 4.

established by Dziembowski & Goode (2004):

$$\left(\frac{\delta\nu}{\nu}\right)_l = -\frac{3l}{2\omega^2 I}\int dI \frac{g}{r}\frac{\delta r}{r} \tag{3.1}$$

where l is the degree of the f-modes, I is the moment of inertia, ω is the pulsation and g is the gravity acceleration. This equation is the starting point for our inversion that will permit us to obtain the variation of the position of the subsurface layers, δr, from $\delta\nu/\nu$. M_1 is the reference model and the inversion procedure is the standard Regularized Least-Square technique (Tikhonov & Arsenin 1977). The inversion of Eq. 3.1 for each model leads to the solutions plotted in Fig. 4[2]. We have checked that the reconstructed frequencies obtained by integration of these solutions through Eq. 3.1 fit pretty well the trend of the real frequencies within the errorbars (Fig. 5), which are fixed artificially at 1×10^{-6}. The main characteristics of our solution are:

1. Fig. 4 shows constant variations below $0.98R_\odot$ and non-monotonic changes in the stratification with a bump centered at $0.99R_\odot$.

[2]Note that the solution is not unique: an other solution exists with other regularisation parameters but leads to variations at the surface not in agreement with the theoretical variation of radius as cited in Table 1.

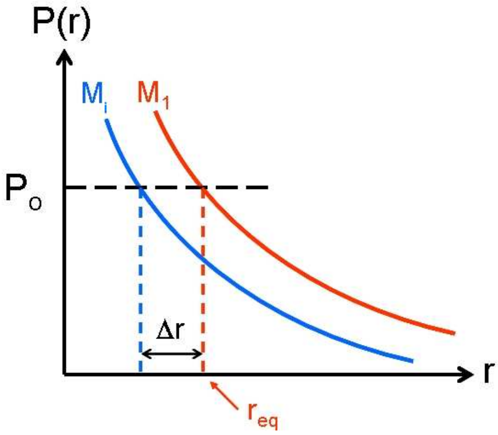

Fig. 6. Scheme explaining the procedure to compute the variation of radius needed to stay on the same iso-surface concerning a quantity P and for each model M_i, i=2...5. P_o is here the chosen value of the iso-P surface. r_{eq} is the equilibrium radius of the f-mode that probes this depth.

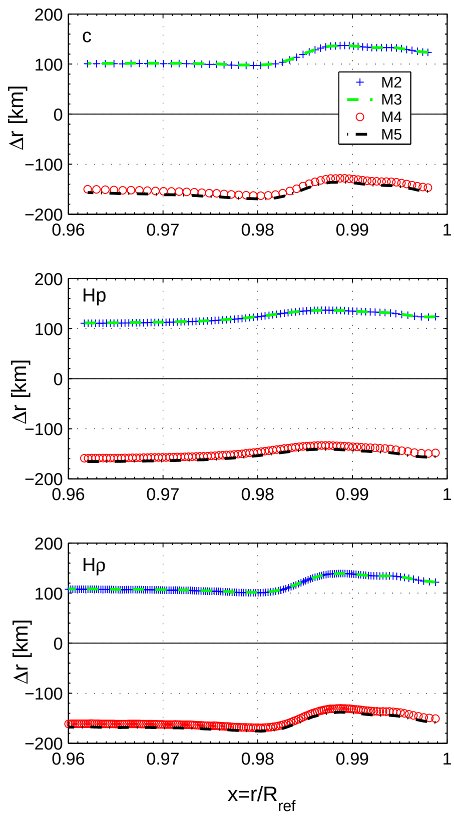

Fig. 7. Computed variation of the radius by the procedure explained in Fig. 6 for the quantities c, H_ρ and H_p and for each model M_i, i=1...5. The reference is as usual M_1. Note that this Δr has also been computed for the other parameters, but the only parameters showing a probant link with the f-mode equilibrium radius is c, H_ρ and H_p.

2. These variations are different in shape (and of course in amplitude) to the ones found by Lefebvre & Kosovichev (2005). But the problem here is also different as in this first approach, we used models without differential rotation nor magnetic field, contrary to the reality.
3. The amplitude for the difference in radius at the surface is similar to that pf the total radius, i.e. about 140 km.

Following this result, we have searched to understand the link of these variations with the physical process in the subsurface layers.

4 Related physics

The goal here is to understand what influences the position of the equilibrium radius, around which the f-mode (analogous to a surface wave) propagates. We have thus calculate the variation of radius needed for each parameter to return to its reference state. The procedure is explained in Fig. 6. If P is the considered parameter (mass, temperature, etc...), P is a function of the radius r. If M_1 is the reference model, and M_i the perturbed model, then by choosing a range of values P_o for this parameter P, we can calculate the variation of radius Δr needed to stay on the same isosurface, i.e. the iso-P, whose value here is P_o. Hence, we obtained results in Fig. 7 where Δr is plotted versus the fractional radius x, for the quantities c, H_ρ and H_p. Our results show:

1. The very good agreement between Figs. 7 and 4, in shape and in amplitude, demonstrates that the f-mode frequencies are directly related to the pressure scale height and indirectly to the density scale height and

the sound speed, because these three quantities are linked by the Γ_1 factor in the adiabatic part of the Sun. We deduced that f-mode frequencies are mainly sensitive to the pressure (or density) scale height. This can be understood when recalling that a surface wave is a wave at a discontinuity of pressure and density, discontinuity relatively to its wavelenght. Thus the equilibrium radius of a surface wave must be dictated by a value of a pressure or density scale height.

2. The order of magnitude between $\Delta\nu/\nu$ plotted in Fig. 5 (10^{-4}) and Δr (100 km) is compatible with real frequencies and radius variations of about respectively 10^{-5} and 10 km or less.

We have also applied the same procedure to the other parameters. But the variations of Δr obtained, not plotted here, are completely different from the one computed by inversion of f-mode frequencies.

5 Conclusions and perspectives

According these results, we show in this paper that a variation in the solar radius produces changes in the subsurface dynamical processes that are in the same zone than that studied by Lefebvre & Kosovichev (2005). This dynamics is characterized by changes in the subsurface stratification and more exactly variations in the computed seismic position of the layers. These changes are physically related to the variation of the pressure scale height. To investigate further, the next step will be to analyse more realistic models including magnetic field. Finally, we underline that a better knowledge of these subsurface layers is necessary to understand (i) the dynamics of the solar cycle and (ii) the Sun-Earth relashionships for space weather but also for space climate. This study is in the perfect framework of coming future space missions: perspective of SDO (see http://sdo.gsfc.nasa.gov/), PICARD (see http://smsc.cnes.fr/PICARD/) in the next future. The DynaMICCS project (Turck-Chièze et al. 2006), proposed in the framework of ESA Cosmic Vision, will put together complementary instruments to gather precise data to follow, among others objectives, these subsurface layers.

S. Lefebvre is supported by a CNES/GOLF postdoctoral grant in SAp.

References

Christensen-Dalsgaard, J. 1982, MNRAS, 199, 735

Couvidat, S., Turck-Chièze, S., & Kosovichev, A. G. 2003, ApJ, 599, 1434

Dziembowski, W. A., & Goode, P. R. 2004, ApJ, 600, 464

Godier, S., & Rozelot, J. P. 2001, Sol. Phys., 199, 217

Lefebvre, S., & Kosovichev, A. G. 2005, ApJ, 633, L149

Lefebvre, S., Kosovichev, A. G., & Rozelot, J. P. 2007, ApJ, 658, L135

Morel, P. 1997, A&AS, 124, 597

Nghiem, P. A. P., García, R. A., & Jiménez-Reyes, S. J. 2006, in ESA-SP 624, Proceedings of SOHO 18/GONG 2006/HELAS I: Beyond the spherical Sun, eds. K. Fletcher & M. Thompson, Published on CDROM, 70.1

Rozelot, J. P., et al. 2006, Solar and heliospheric origins of space weather phenomena, ed. J.-P. Rozelot (Springer press, Berlin Heidelberg), Lect. Notes Phys., 699

Tikhonov, A. N., & Arsenin, V. Y. 1977, Solutions of ill-posed problems, Washington D. C.: Winston

Turck-Chièze, S., et al. 2001, ApJ, 555, L69

Turck-Chièze, S., et al. 2006, in ESA-SP 624, Proceedings of SOHO 18/GONG 2006/HELAS I: Beyond the spherical Sun, eds. K. Fletcher & M. Thompson, Published on CDROM, 24.1